

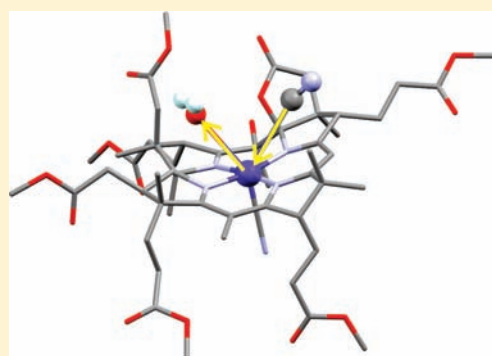
Probing the Nature of the Co^{III} Ion in Corrins: A Comparison of the Thermodynamics and Kinetics of the Ligand Substitution Reactions of Aquacyanocobyrinic Acid Heptamethyl Ester and Stable Yellow Aquacyanocobyrinic Acid Heptamethyl Ester

Susan M. Chemaly,^{*,†} Melissa Florczak,[†] Heinrich Dirr,[‡] and Helder M. Marques^{*,†}

[†]Molecular Sciences Institute, School of Chemistry, and [‡]Protein Structure–Function Unit, School of Molecular and Cell Biology, University of the Witwatersrand, P.O. Wits, Johannesburg, 2050 South Africa

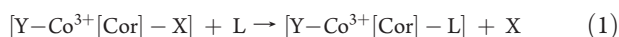
S Supporting Information

ABSTRACT: Equilibrium constants ($\log K$) for the substitution of coordinated H₂O in aquacyanocobyrinic acid heptamethyl ester (aquacyanocobester, ACCbs) and stable yellow aquacyanocobyrinic acid heptamethyl ester (stable yellow aquacyanocobester, ACSYCbs), in which oxidation of the C5 carbon of the corrin interrupts the normal delocalized system of corrins, by ligands with soft (CN⁻, SO₃²⁻, and S₂O₃²⁻) and hard (NO₂⁻ and N₃⁻) donors have been determined. The ligands with a harder donor atom (N in N₃⁻ and NO₂⁻) produce ΔH values that are more negative in their reactions with ACSYCbs than with ACCbs. If the donor atom is softer (C in CN⁻ and S in SO₃²⁻), then ΔH is less positive, or more negative, for reactions with ACCbs than with ACSYCbs. The softer metal in ACCbs has a preference for softer ligands and the harder metal in ACSYCbs for the harder ligands. A kinetics study in which CN⁻ substitutes H₂O on Co^{III} shows that ACCbs is more labile than ACSYCbs; the second-order rate constant k^{II} is between 4.6 (at 5 °C) and 2.6 (at 35 °C) times larger. ΔH^{\ddagger} for the reaction of CN⁻ with ACCbs is smaller by some 12 kJ mol⁻¹ than that for the reaction with ACSYCbs, consistent with an earlier transition state in which bonding between the softer metal of ACCbs and the ligand is greater than that of ACSYCbs with its harder metal. This difference in ΔH^{\ddagger} makes ACCbs over 100 times more labile, although the effect is masked by a ΔS^{\ddagger} value that is over 30 J K⁻¹ mol⁻¹ more negative. There is a significant increase in the inertness of Co^{III} upon a decrease in the extent of conjugation of the corrin ligand. Modifying the electronic structure of the equatorial ligand in the cobalt corrins can modify the thermodynamics and kinetics of its reactions with exogenous ligands.



INTRODUCTION

We are interested in how perturbation of the electronic structure of the corrin ligand affects the ligand binding properties of the metal ion in order to explain why cobalt(III), a normally inert metal ion, is labile in the corrins (see the Introduction to the accompanying paper¹). We have examined the thermodynamics and kinetics of the ligand substitution reactions of the aquacyano (AC) complexes of the cobesters (eq 1), where [Cor] is the normal corrin ligand in ACCbs (Cbs = cobyrinic acid heptamethyl ester, or cobester) and the stable yellow (SY) corrin in ACSYCbs.



We converted the dicyano complexes DCSYCbs (Figure 1) and DCCbs to the corresponding aquacyano complexes and determined the stability constants for replacement of coordinated H₂O by ligands with soft (CN⁻, SO₃²⁻, and S₂O₃²⁻) and hard (NO₂⁻ and N₃⁻) donor atoms as a function of the temperature,

from which ΔH and ΔS for ligand substitution were determined. We found that the rate of reaction with L = N₃⁻ was too fast to study by conventional stopped-flow methods but that the reaction with L = CN⁻ proceeds at a convenient rate for this technique. The kinetics were measured as a function of the temperature from which we determined values of ΔH^{\ddagger} and ΔS^{\ddagger} . The kinetics of the reaction of diaquacobester (DACbs; eq 1, X = Y = H₂O, with L = CN⁻ at 25 °C) were also determined.

Aquacyano derivatives of vitamin B₁₂ complexes lacking the 5,6-dimethylbenzimidazole side chain are well-known to exist in solution as two diastereomers, α -cyano, β -aqua and β -cyano, α -aqua, in equilibrium with each other.^{2–5} The existence of diastereomers inevitably complicated the study of the equilibria and kinetics of ACCbs and ACSYCbs.

Received: February 10, 2011

Published: August 18, 2011

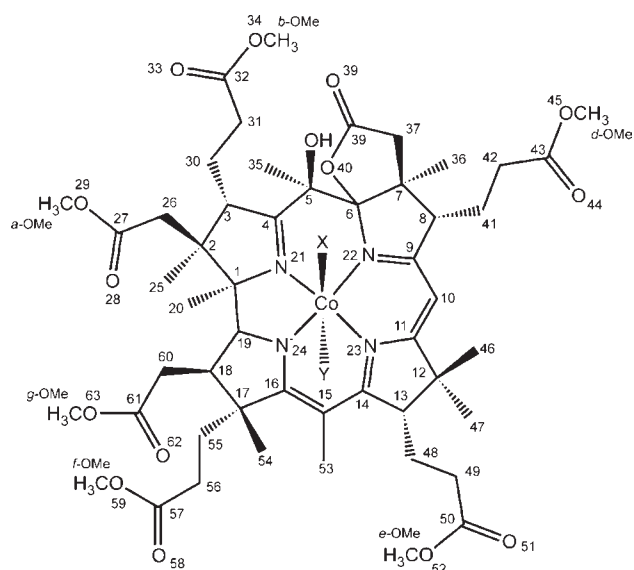


Figure 1. Structure of the stable yellow dicyanocobester, (5*R*,6*R*)-Co α , Co β -dicyano-5,6-dihydro-5-hydroxyheptamethylcob(III)yrinate- ϵ ,6-lactone ($X = Y = \text{CN}^-$, DCSYCbs). The aqua-cyano derivative (ACSYCbs) consists of two interconverting diastereomers, $X = \text{H}_2\text{O}$, $Y = \text{CN}^-$ and $X = \text{CN}^-$, $Y = \text{H}_2\text{O}$.

EXPERIMENTAL SECTION

Materials and Instrumentation. Materials were purchased from the following suppliers and used without further purification: potassium cyanide, BDH (AR); granulated zinc, BDH (CP); sodium azide, Riedel de Haën; sodium bicarbonate and sodium carbonate, Saarchem (Unilab); ammonium bromide, disodium hydrogen phosphate, sodium hydrogen phosphate, sodium nitrite, sodium sulfite, and sodium sulfate pentahydrate, Saarchem (AR). Water was purified using a Millipore RO unit and further purified using a Millipore Milli-Q unit (18 M Ω cm). The C18 Sep-Pak Vac columns were purchased from Waters.

High-performance liquid chromatography (HPLC) was performed using an Ultimate 3000 pump and a photodiode array detector with Chromoleon Chromatographic Management System software and a reverse-phase C18 column (Phenomenex Luna C18 5 μ , 150 \times 4.60 mm), using gradient elution with ammonium phosphate buffer pH 3.0, 0.025 M (100%) to methanol (100%) over 15 min or isocratic elution with methanol; flow rate 1 mL min $^{-1}$ (350 bar).

UV-vis spectra were recorded in 10-mm-path-length quartz cuvettes on a Cary 1E or Cary 300 UV-vis spectrophotometer. Reaction kinetics were measured by absorption spectrophotometry using a stopped-flow spectrophotometer with a dead time of 2 ms (SX-18MV, Applied Photophysics; a SpectraKinetics 05-109 monochromator set at a bandwidth of 0.5 nm and a 2-mm-path-length cell). ACCbs, initially at 6.14 $\times 10^{-5}$ M and ACSYCbs, initially at 3.60 $\times 10^{-5}$ M, in carbonate buffer, pH 9.6, $\mu = 0.1$ M, were diluted (5:1) with potassium cyanide dissolved in the same buffer (six solutions with final free [CN $^-$] between 0.25 and 2.5 mM, taking into account the pH and temperature dependence of the ionization of HCN, $^6 \Delta H = -43.9$ kJ mol $^{-1}$, and $\Delta S = 24.3$ J K $^{-1}$ mol $^{-1}$). DACbs, initially at 5.17 $\times 10^{-5}$ M in water (pH \sim 5.5 from dissolved CO $_2$), was diluted (1:5) with potassium cyanide dissolved in carbonate buffer, $\mu = 0.6$ M, to give six solutions with final free [CN $^-$] between 1.33 and 13.3 mM in carbonate buffer, pH 9.0, $\mu = 0.5$ M. DACbs was dissolved in water rather than in carbonate buffer because of its instability at basic pH (see below). No decomposition of DACbs in water (pH \sim 5.5) was observed during the time of the stopped-flow experiment (about 3 h). The temperature of

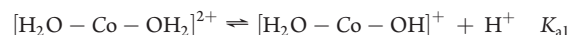
the cell block of the spectrometer and the solution chamber of the stopped-flow spectrophotometer were maintained (± 0.1 $^\circ\text{C}$) by a water-circulating bath and measured with a thermistor device. The pH was measured using a Metrohm 720 or 827 pH meter with a Unitrode or Biotrode electrode calibrated at pH 7.00 and 9.00 with standard buffers.

Attempts To Separate the Diastereomers of ACCbs and ACSYCbs. Attempts to separate the diastereomers of ACCbs and ACSYCbs on a 10 g C18 Sep-Pak column by elution with water and methanol were unsuccessful and gave inconsistent results. Sometimes two bands, red for ACCbs and yellow for ACSYCbs, with varying degrees of overlap were obtained and sometimes only one broad band. Usually, small amounts of the purple dicyanocobester were also observed.

NMR. One-dimensional ^1H NMR was carried out on a Bruker Biospin GmbH 500 MHz spectrometer using a broad-band inverse probe at 300 K.

Preparation and Characterization of Co α ,Co β -Diaquaheptamethylcob(III)yrinate Heptamethyl Ester (Diaquacobester, DACbs). To DCCbs (54 mg) dissolved in 25 mL of methanol was added 1.25 g of ammonium bromide, and the solution was stirred under argon for 1 h. Granulated zinc (710 mg) was added and a stream of argon passed through for 2.5 h, during which time the solution darkened in color, becoming almost black. The reaction mixture was added to 1 M HCl, turning red immediately, and filtered. 7 The solution was desalted on a 1 g C18 Sep-Pak column, by washing with water until the pH was neutral, and then eluted with 20:80 acetone/water. After rotary evaporation (maximum temperature 50 $^\circ\text{C}$), the concentrated aqueous solution was stored at -20 $^\circ\text{C}$. 8 The yield of DAC was only about 30% because a substantial proportion of the product degraded on the C18 column and could not be removed from it, even with pure acetone. DACbs was characterized and its purity checked by comparing its UV-vis spectrum at pH 2.8 [λ/nm ($\times 10^{-4}$, $\epsilon/\text{L mol}^{-1} \text{cm}^{-1}$) 518 (0.97), 490 (0.97), 401 (0.40), 348 (2.96)] to that of diaquacobinamide (DACbi). $^{8-10}$

Attempt To Determine the p*K* $_a$ of DACbs. The acid dissociation constants, p*K* $_{a1}$ and p*K* $_{a2}$, for the two coordinated water molecules in DACbs are given in eq 2.



For DACbi, the values of p*K* $_{a1}$ and p*K* $_{a2}$ are 5.9 and 10.3, respectively. 7,9,10 For DACbs, the values of p*K* $_{a1}$ and p*K* $_{a2}$ could not be determined because DACbs was found to be unstable in a basic solution, as previously observed by Hamza, 11 and the rate of decomposition increased with increasing pH. At pH 12.0, a product with the UV-vis spectrum [λ/nm ($\times 10^{-4}$, $\epsilon/\text{L mol}^{-1} \text{cm}^{-1}$) 531 (1.05), 507 (1.05), 416 (0.39), 354 (2.17)] is obtained, which can be ascribed to hydrolysis of one or more of the ester side chains in DACbs, as described in the accompanying paper for ACCbs and ACSYCbs. 1

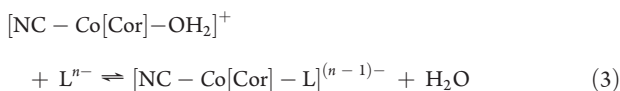
Effect of pH on ACCbs, ACSYCbs, and DACbs. As reported in the accompanying paper, 1 we estimate the p*K* $_a$ of ACCbs and ACSYCbs as \sim 11. Because pH 9.6 was the highest pH used for determining equilibrium constants (vide infra) or the kinetics of the ligand substitution reaction with CN $^-$, correction for the hydrolysis of coordinated H $_2$ O in either ACCbs or ACSYCbs is unnecessary. Assuming that p*K* $_{a1}$ and p*K* $_{a2}$ for DACbs are similar to those for DACbi, viz., 5.9 and 10.3, respectively, 7,9,10 at pH 9.6, DACbs consists of 83.4% of the [H $_2$ O-Co-OH] $^+$ form and 16.6% of the [HO-Co-OH] form. It is therefore reasonable to assume that reactions of DACbs studied at pH 9.0–9.6 are the reactions of aquahydrocobester (AHCbs).

Molecular Modeling. Molecular mechanics (MM) calculations were performed with the version of Allinger's MM2 12 program implemented in Hyperchem 13 (called MM *) together with the force field that we have reported 14 and that accurately models the structures of cobalt corrins. 15 Molecular dynamics/simulated annealing calculations

were performed by heating the molecule from 0 to 600 K over 5 ps in steps of 1 fs, maintaining the temperature at 600 K for 500 ps, and annealing to 0 K over 100 ps, followed by energy minimization with a convergence criterion of 0.005 kcal mol⁻¹ Å⁻¹ in the gradient. The volumes of the ions SO₃²⁻ and S₂O₃²⁻ were determined from an energy-minimized structure obtained with the semiempirical PM3 model¹⁶ using the grid method described by Bodor et al.¹⁷ and the atomic radii of Gavezotti,¹⁸ as implemented in *Hyperchem*.¹³

Equilibrium Constants. The equilibrium constants for coordination of the ligands by ACCBs and ACSYCbs were determined by the addition of aliquots of a stock solution of the appropriate ligand to a 20–30 μM solution of cobalt corrin contained in a 10-mm-path-length cuvette housed in the thermostatted cell block of a UV–vis spectrophotometer. Between 12 and 18 aliquot additions were made in each titration. All absorbance readings were corrected for dilution. The solutions were buffered with phosphate (pH 8, for titrations with N₃⁻, NO₂⁻, and S₂O₃²⁻) or carbonate (pH 9, for titrations with CN⁻ and SO₃²⁻) at an ionic strength μ = 0.10 M.

By analogy with the cobinamides (Cbi's),¹⁹ and as can be seen by HPLC [and thin layer chromatography (TLC) for ACCBs], both ACCBs and ACSYCbs exist as an equilibrium of two diastereomers in solution, viz., α-cyano,β-aqua and β-cyano,α-aqua. These are expected to have similar, but not identical, equilibrium constants (log *K*, eq 3) for replacement of coordinated H₂O by an exogenous ligand L.



The binding constants for the addition of cyanide to the α and β forms of base-off cyanocobalamin²⁰ are 2.1 × 10⁸ and 0.8 × 10⁸ M⁻¹, respectively. One would expect the equilibrium constants for the two diastereomers of ACCBs to be even more similar because the upper and lower sides of the corrin are more similar to each other than those of base-off cyanocobalamin. Moreover, our equilibrium constants are conditional binding constants at a defined, buffered pH, whereas those for the addition of cyanide to the α and β forms of base-off cyanocobalamin are not.

In such situations, a spectrophotometric determination of log *K* will show a wavelength dependence, which is a function of the relative extinction coefficients of the two diastereomers at the monitoring wavelength.²¹ Therefore, we determined log *K* at every 1 or 2 nm between about 320 and 570 nm, excluding wavelengths (such as those close to isosbestic points) where the absorbance change was small. Figure S1 in the Supporting Information shows examples of the spectral changes accompanying the coordination of N₃⁻ by ACCBs and ACSYCbs.

For cases where log *K* is relatively small (log *K* < 4), the absorbance data at wavelength λ were fitted using nonlinear least-squares methods with *SigmaPlot*²² to a simple binding isotherm (eq 4) as the objective function, with A₀, A₁, and *K* as the parameters to be optimized. A₀ and A₁ are the absorbance values at λ corresponding to 0 and 100% complex formation, respectively.

$$A_\lambda = (A_0 + KA_1[L]) / (1 + K[L]) \quad (4)$$

When log *K* is relatively large (>4), the implicit assumption in eq 3 that [L]_{free} ≈ [L]_{total} will not be true because a significant fraction of the added ligand will be complexed to the metal ion. In this case, [L] in eq 4 has to be replaced by an explicit expression for [L]_{free}. It can be shown²³ that [L]_{free} is given by eq 5, where only one root has physical meaning. In eq 5, [M]_{total} is the total metal ion concentration.

$$[\text{L}]_{\text{free}} = \frac{-a_2 \pm \sqrt{a_2^2 - 4a_1a_3}}{2a_1} \quad a_1 = K; \\ a_2 = 1 + K[\text{M}]_{\text{total}} - K[\text{L}]_{\text{total}}; \quad a_3 = -[\text{L}]_{\text{total}} \quad (5)$$

Only values of log *K* obtained from fits for which the correlation coefficient *r*² > 0.97 were accepted. *K* was then found from a weighted average, weighted by the reciprocal of the variance, 1/σ², where the standard deviation σ = (standard error of the fit)/*n*^{1/2} for *n* data points in the titration.

log *K* for binding of CN⁻ was expected to be large; the value was therefore determined in a competition experiment in the presence of 1.2 M N₃⁻. Under these conditions, there is >99% formation of the azidocyanide complex. *K* for binding of CN⁻ was determined from *K*_{cyanide} = *K*_{obs}*K*_{azide}, where *K*_{obs} is the observed equilibrium constant for binding of CN⁻ in the presence of excess N₃⁻. The values were corrected for the p*K*_a of HCN.⁶ It was unnecessary to correct values for the p*K*_a of N₃⁻ (p*K*_a = 4.4; pH of determination of *K* = 8), NO₂⁻ (p*K*_a = 2.94; pH 8), SO₃²⁻ (p*K*_a = 1.66 and 6.85; pH 9), or S₂O₃²⁻ (p*K*_a = 0.6 and 6.12; pH 8).

Values of *K* were determined as a function of the temperature between 10 and 40 °C. For titrations of ACSYCbs with SO₃²⁻, however, we were limited to *T* < 30 °C as the ligand slowly reduces cobalt(III) and the solution becomes turbid. Above 30 °C, this process is too rapid for the reliable determination of log *K* values. Values of Δ*H* and Δ*S* were determined from the slope and intercept, respectively, of weighted linear least-squares van't Hoff plots of ln *K* against 1/*T*.

Rate Constants. We examined the change of absorbance of ACCBs upon the addition of CN⁻ at 353, 368, 497, 540, and 579 nm under pseudo-first-order conditions ([CN⁻] > 5–50 × [cobester]) in sodium carbonate buffer, pH 9.5 (25 °C), μ = 0.10 M. In each case, the absorbance/time trace is clearly biphasic (Figure S2 in the Supporting Information). The data were therefore fitted to a double-exponential function (eq 6).

$$A = A_0 + ae^{-k_1t} + be^{-k_2t} \quad (6)$$

Because, within experimental error, the values of the two pseudo-first-order rate constants *k*₁ and *k*₂ did not depend on the monitoring wavelength (see below), all data were collected at 368 nm for the reaction of ACCBs with CN⁻ and at 478 nm for the reaction of ACSYCbs with CN⁻ at five temperatures between 5 and 35 °C. Each reaction was repeated five times, and the average values of *k*_{*j*}, where *j* = 1 and 2, were used to determine the corresponding second-order rate constants *k*₁^{II} and *k*₂^{II} from weighted linear least-squares plots of *k*_{*j*} against [CN⁻], where *j* = 1 and 2. Values of Δ*H*[‡] and Δ*S*[‡] were determined from weighted linear least-squares Eyring plots of ln(*k*_{*j*}^{II}*h*/*k*_B*T*) against *T*⁻¹, where *h* and *k*_B are the Planck and Boltzmann constants, respectively.

For DACBs, we examined the change of absorbance upon the addition of CN⁻ in sodium carbonate buffer, pH 9.0, μ = 0.5 M, at 25 °C and 367 nm under the same conditions as those for ACCBs and ACSYC. The absorbance/time trace appears to be monophasic, and the data were fitted to a single-exponential function. Each reaction was repeated at least five times, and the average value of *k* was used to determine the corresponding second-order rate constant *k*^{II} from weighted linear least-squares plots of *k* against [CN⁻].

RESULTS

HPLC. HPLC of ACCBs on a C18 column, gradient elution with phosphate buffer, pH 3, and methanol, shows two peaks at 1.9 min (58%) and 4.4 min (42%). HPLC of ACSYCbs on a C18 column, isocratic elution with methanol, shows two poorly resolved peaks at 2.4 min (91%) and 2.7 min (9%); gradient elution with phosphate buffer, pH 3, and methanol gives similar results, two poorly resolved peaks at 2.4 min (93.5%) and 2.8 min (6.5%). Both ACCBs and ACSYCbs showed tailing of the peaks, which strongly suggests that interconversion of isomers and/or decomposition on the column is taking place during the separation.

^1H NMR of ACCbs. The ^1H NMR spectrum of ACCbs in CD_3OD at 300 K shows a peak at 6.46 ppm, which we assign to the C-10 proton by comparison with the ^1H NMR spectra of ACCbi in CD_3OD ²⁴ and D_2O .²⁵ The peak is asymmetrical and very broad (about 0.5 ppm at its base), which suggests that it comprises two peaks due to the C-10 protons of the two diastereomers in an approximately 2:1 ratio and that there is rapid (on the NMR time scale) equilibration between them. The rest of the ^1H NMR spectrum is complex, and no certain assignments could be made. Krätler et al.²⁶ reported that β -aqua, α -cyanocobyrinic acid equilibrated to a mixture of α -aqua, β -cyano- and β -aqua, α -cyanocobyrinic acid upon dissolution in D_2O for ^1H NMR spectroscopy and that “for practical reasons” NMR was not carried out on this compound but only on dicyanocobyrinic acid.

MM Modeling. In the accompanying paper,¹ we noted that O40 of the c_6 ,6-lactone in DCSYC comes close to the β - CN^- ligand [the $\text{O40}\cdots\text{C}(\beta\text{-CN}^-)$ distance is 2.92 Å for a van der Waals overlap of $\sigma_{\text{vdW}} = 0.30$ Å; we have used van der Waals’ radii as recommended by the CCDC, which may be obtained at <http://www.ccdc.cam.ac.uk/products/csd/radii/table.php4>]. This could lead to a marginal lengthening of the Co–CN bond length, but it has no effect on the CN–Co–CN angle. We have endeavored to gauge the steric effect of the c_6 ,6-lactone on complexes of SYCbs with $\text{L} = \text{N}_3^-$, NO_2^- , SO_3^{2-} , and $\text{S}_2\text{O}_3^{2-}$, ligands pertinent to this work, by performing MM/simulated annealing calculations on the α -cyano, β -L stable yellow cobester and examining the resultant structures (Figure S3 in the Supporting Information).

N_3^- coordinates in a bent fashion, oriented over C15. The Co– N_3 bond length in the model is 1.977 Å, in good agreement with 1.984 Å observed in the crystal structure of N_3Cbl .²⁷ There is contact between O40 and N_α of coordinated azide ($d = 2.57$ Å; $\sigma_{\text{vdW}} = 0.50$ Å). C26H, C19H, C46H, and C54H are close to coordinated N_3^- , although only C19H makes contact (with N_α ; $d = 2.49$ Å; $\sigma_{\text{vdW}} = 0.15$ Å).

In (α -CN, β - NO_2)SYCbs, the Co– NO_2 bond length is 1.954 Å, also in reasonable agreement with that observed in NO_2Cbl (1.940 Å with solvent acetone included in the lattice,²⁸ 1.942 Å with lithium chloride, and much shorter at 1.913 Å with sodium chloride included in the lattice²⁹). O40 makes a short contact with one of the NO_2 O atoms ($d = 2.45$ Å; $\sigma_{\text{vdW}} = 0.59$ Å), and C26H contacts the same O atom ($d = 2.30$ Å; $\sigma_{\text{vdW}} = 0.31$ Å). The NO_2 ligand is bent ($\text{NC–Co–NO}_2 = 173.0^\circ$) toward the “southern” quadrant.

The Co–S bond length in the energy-minimized structure of stable yellow sulfitecyanocobester is 2.243 Å (cf. 2.230³⁰ and 2.241³¹ Å in SO_3Cbl^-). There is contact between O40 and an O atom of coordinated SO_3 ($d = 2.60$ Å; $\sigma_{\text{vdW}} = 0.44$ Å), but the most severe contact is between C26H and a ligand O ($d = 2.22$ Å; $\sigma_{\text{vdW}} = 0.67$ Å), while C19H also makes close contact ($d = 2.56$ Å; $\sigma_{\text{vdW}} = 0.33$ Å). In the thiosulfato complex, the Co–S bond length is 2.243 Å (2.2870 Å²⁸ in $\text{S}_2\text{O}_3\text{Cbl}^-$).

In all cases, steric interactions between O40 and the coordinated ligand do not appear to unduly perturb the metal–ligand bond. We therefore expect them to have at most a small effect on the ligand binding properties of the α -CN, β - H_2O -SYCbs and, of course, no effect on the other diastereomer.

Equilibrium Constants. Examples of fits of absorbance as a function of the ligand concentration to eq 4 (for N_3^-) and eq 5 (for CN^-) are shown in Figure S4 in the Supporting Information. Applying eq 5 to the data for N_3^- binding gave essentially

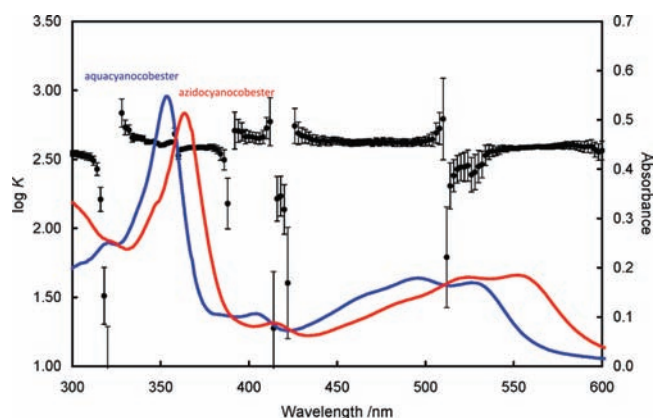


Figure 2. Wavelength dependence of $\log K$ (circles, with standard error bars, left axis) for substitution of H_2O by N_3^- in ACCbs (pH 9.07, 24.4 °C). Values of $\log K$ are particularly sensitive to the monitoring wavelength near isosbestic points, where errors increase significantly. The spectrum (right axis) of ACCbs is shown in blue and that of its azido complex (N_3^- replaces H_2O) in red.

the same value of $\log K$. As discussed above, the values of $\log K$ are expected to depend on the monitoring wavelength; this is indeed the case, as illustrated in Figure 2 for N_3^- as an example. As explained in the Experimental Section, only those wavelengths that gave $r^2 > 0.97$ and that were away from the isosbestic points (2 or 3 nm in the UV region, where the absorbance change with the wavelength is larger, and 3–5 nm in the visible region, where it is smaller) were used for acquiring data. Typically, between 100 and 200 wavelengths were used per titration to obtain a weighted $\log K$ average value. These weighted $\log K$ values are listed in Table 1. The value of K for coordination of $\text{S}_2\text{O}_3^{2-}$ by ACSYCbs was too small for a reliable determination. At 25 °C, the only temperature at which a measurement was attempted, we found $K = 0.6 \pm 0.2 \text{ M}^{-1}$. An example of a van’t Hoff plot obtained for the data in this work is shown in Figure S5 in the Supporting Information.

Rate Constants. The substitution of coordinated H_2O in both ACCbs and ACSYCbs by CN^- is biphasic (Figure S2 in the Supporting Information); the values of the two pseudo-first-order rate constants k_1 and k_2 do not depend on the monitoring wavelength (Table S1 in the Supporting Information). The values of the second-order rate constants k_1^{II} and k_2^{II} , together with the values of ΔH^\ddagger and ΔS^\ddagger determined from their temperature dependence, are given in Table 2, while the full kinetic data are given in Table S2 in the Supporting Information. An example of a plot of k_1 and k_2 against $[\text{CN}^-]$ is given in Figure S6 in the Supporting Information, while the Eyring plots are given in Figure S7 in the Supporting Information.

The substitution of coordinated H_2O in AHCbs by CN^- appears to be monophasic. The value of the second-order rate constant, k^{II} , is given in Table 2, while the full kinetic data are given in Table S2 in the Supporting Information.

DISCUSSION

Presence of Diastereomers. The HPLC of ACCbs shows the presence of two interconverting species in an approximately 2:1 ratio; these are presumably the α -cyano, β -aqua and β -cyano, α -aqua diastereomers. This is supported by the presence in the ^1H NMR spectrum of an asymmetrical broad peak, due to the

Table 1. Equilibrium Constants for the Substitution of Coordinated H₂O in ACCbs and ACSYCbs by Some Anionic Ligands^a

ligand	ACCbs					ACSYCbs				
	<i>T</i> / °C	<i>K</i> / M ⁻¹	log <i>K</i>	ΔH / kJ mol ⁻¹	ΔS / J K ⁻¹ mol ⁻¹	<i>T</i> / °C	<i>K</i> / M ⁻¹	log <i>K</i>	ΔH / kJ mol ⁻¹	ΔS / J K ⁻¹ mol ⁻¹
N ₃ ⁻	9.6	459(21)	2.662(19)	-9.4(7)	18(3)	9.9	634(36)	2.80(2)	-18.6(7)	-12(2)
	17.0	425(6)	2.628(6)			16.7	544(40)	2.74(3)		
	24.4	394(9)	2.595(10)			23.2	440(35)	2.64(3)		
	31.8	355(12)	2.550(14)			29.9	373(32)	2.57(4)		
	39.2	315(9)	2.498(12)			37.4	320(23)	2.51(3)		
CN ⁻	9.6	2.5(7) × 10 ⁸	8.19(11)	-23(2)	81(6)	9.9	1.6(2) × 10 ⁷	7.20(5)	-17(1)	80(5)
	17.0	1.9(3) × 10 ⁸	8.08(6)			16.7	1.4(2) × 10 ⁷	7.13(5)		
	24.4	1.5(4) × 10 ⁸	8.10(10)			23.2	1.25(15) × 10 ⁷	7.10(5)		
	32.5	1.3(4) × 10 ⁸	8.06(11)			29.9	9.9(1.2) × 10 ⁶	7.00(5)		
	40.0	9(2) × 10 ⁷	7.88(8)			37.4	8.5(1.5) × 10 ⁶	6.93(7)		
NO ₂ ⁻	9.9	844(23)	2.93(1)	-6.6(9)	33(3)	9.9	372(12)	2.57(1)	-22.9(4)	-32(2)
	16.7	813(22)	2.91(1)			16.7	290(10)	2.46(2)		
	23.2	778(21)	2.89(1)			23.2	238(7)	2.38(1)		
	29.9	728(31)	2.86(2)			29.9	192(6)	2.28(1)		
	37.4	653(23)	2.81(1)			37.4	158(8)	2.20(2)		
SO ₃ ²⁻	9.9	5.0(3) × 10 ⁴	4.70(3)	50(3)	265(9)	9.9	232(14)	2.37(3)	59(1)	253(5)
	16.7	7.4(3) × 10 ⁴	4.87(2)			16.7	365(42)	2.56(5)		
	23.2	10.0(4) × 10 ⁴	5.00(2)			20.5	673(39)	2.83(3)		
	29.9	12.9(8) × 10 ⁴	5.11(3)			23.2	1144(57)	3.06(2)		
	37.4	19(1) × 10 ⁴	5.29(3)			29.2	2063(61)	3.31(1)		
S ₂ O ₃ ²⁻	9.9	2.15(9)	0.33(2)	21(3)	80(10)	23.2	0.6(2)	-0.2(1)		
	16.7	2.3(1)	0.37(2)							
	23.2	3.3(3)	0.51(4)							
	29.9	3.6(3)	0.56(4)							
	37.4	4.8(1)	0.7(2)							

^a These are conditional binding constants, at the pH of the determination (see the Experimental Section). However, they have been corrected for the p*K*_a of the ligand. Correction for the p*K*_a of coordinated H₂O is probably unnecessary (see the text).

Table 2. Second-Order Rate Constants and Activation Parameters for the Substitution of Coordinated H₂O in ACCbs, ACSYCbs, and AHCbs with Cyanide

temp/°C	<i>k</i> ₁ ^{II} /M ⁻¹ s ⁻¹ (×10 ⁴)	ΔH^\ddagger /kJ mol ⁻¹	ΔS^\ddagger /J K ⁻¹ mol ⁻¹	<i>k</i> ₂ ^{II} /M ⁻¹ s ⁻¹ (×10 ³)	ΔH^\ddagger /kJ mol ⁻¹	ΔS^\ddagger /J K ⁻¹ mol ⁻¹
ACCbs						
5.1(1)	1.32(7)	46(3)	-2(9)	1.5(2)	52(7)	1(24)
9.9(1)	1.57(4)			1.2(1)		
17.4(0)	2.89(8)			2.9(4)		
25.2(0)	4.8(3)			5.1(5)		
34.9(1)	9.1(6)			11.1(6)		
ACSYCbs						
5.3(0)	0.286(4)	57.6(9)	29(3)	0.07(1)	72(5)	50(18)
10.4(1)	0.49(2)			0.18(5)		
17.5(0)	0.87(4)			0.24(9)		
24.6(0)	1.53(2)			0.56(7)		
35.1(1)	3.56(10)			1.7(2)		
AHCbs						
25.0				5.3(3)		

different environments of C10–H in the two diastereomers of ACCbs and the rapid interconversion of the two diastereomers. Similarly, it has been shown by ¹H NMR that the diastereomers

of aquacyanocobyrinic acid are in equilibrium in a D₂O solution;²⁶ however, the diastereomers of ACCbi do not interconvert on the NMR time scale.²⁵ It is possible that the presence of the isopropyl

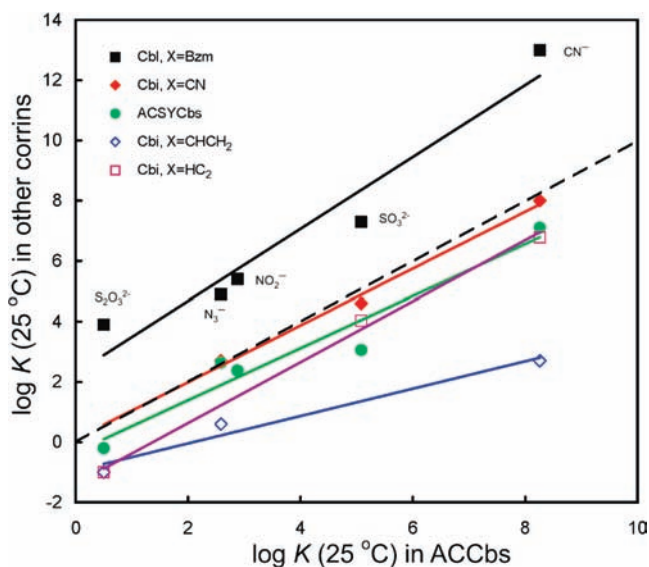


Figure 3. Correlation between $\log K$ (~ 25 °C) for substitution of H_2O trans to $\text{X} = \text{CN}^-$ in ACCBs by five anionic ligands and $\log K$ for the same substitution reactions in five other corrins, aquacobalamin (B_{12a} , $\text{X} = 5,6$ -dimethylbenzimidazole); aquacyanocobinamide ($\text{X} = \text{CN}^-$); ACSYCbs itself; aquavincobinamide ($\text{X} = \text{CHCH}_2$); and aquaethylcobinamide ($\text{X} = \text{CCH}$). Data from this work, from Pratt³ and from Betterton.⁹ The broken line is that for a perfect correlation.

alcohol group on the *f* side chain in ACCbi, but not in ACCBs or aquacyanocobyrinic acid, inhibits the rapid interconversion of the diastereomers.

The HPLC of ACSYCbs also shows the presence of two interconverting species, but their ratio is $\sim 9:1$; these are, by analogy with ACCBs, the α -cyano, β -aqua and β -cyano, α -aqua diastereomers of ACCBs. Because the ratio of the diastereomers is larger than that in ACCBs, it appears that the α and β faces differ sterically to a greater extent in ACSYCbs than in ACCBs. Because both ACCBs and ACSYCbs consist of a mixture of diastereomers, the equilibrium and rate constants must be considered as macroscopic rather than microscopic constants.

Equilibrium Constants. Values of $\log K$ ($T \sim 25$ °C, eq 2) for substitution of axially coordinated H_2O in ACCBs for the five ligands studied vary from 8.1(1) for $\text{L} = \text{CN}^-$ to 0.51(4) for $\text{L} = \text{S}_2\text{O}_3^{2-}$ (Table 1) and from 7.10(5) to $-0.2(1)$ for the same ligands in their reaction with ACSYCbs. The trend in $\log K$ for substitution of H_2O in ACCBs parallels that in ACSYCbs ($\text{CN}^- > \text{SO}_3^{2-} > \text{NO}_2^- \approx \text{N}_3^- > \text{S}_2\text{O}_3^{2-}$) as well as in other corrins (see Figure 3). The values of $\log K$ for ACCBs are very close to those for ACCbi.³ Hamza³² compared $\log K$ values for coordination of N_3^- , SO_3^{2-} , and several neutral N-donor ligands by ACCBs and ACCbi and showed that $\log K$ values for coordination of these ligands by the former are slightly smaller than their coordination by the latter (the values differ typically by 0.2–0.3 units); replacement of amides by esters in the side chains of the corrin has very little effect on the ligand binding properties of cobalt(III). For any given ligand (Figure 3), $\log K$ decreases as the trans ligand is varied from Bzm to CN^- to CHCH_2 to CCH, which is an illustration of the well-established trans effect in cobalt corrin chemistry.³ Also evident from Figure 3 is that $\log K$ for replacement of H_2O trans to CN^- is significantly smaller in ACSYCbs than in ACCBs and ACCbi so the metal ion behaves rather differently in the former compared to the latter two.

However, $\log K$ values determined at a single temperature may not always be as informative as is sometimes assumed. There is a significant compensation effect between values of ΔH and ΔS for these ligand substitution reactions (Figure S8 in the Supporting Information); as values of ΔH become more negative and the substitution reaction becomes enthalpically more favorable, values of ΔS tend to become negative and the reaction is entropically less favored. The effect is to level out values of $\log K$ so that underlying effects may not always be evident. For example, the value of $\log K$ for substitution of H_2O by N_3^- in ACCBs near 25 °C [2.60(1)] is statistically identical with that for the same reaction with ACSYCbs [2.64(3)], but the thermodynamic parameters are very different; ΔH is significantly less negative for the first reaction [$-9.4(7)$ kJ mol⁻¹] than for the second [$-18.6(7)$ kJ mol⁻¹] while, conversely, ΔS is much more positive (18(3) vs $-12(2)$ J K⁻¹ mol⁻¹). It is unfortunate that $\log K$ values in cobalt corrin chemistry have seldom been reported as a function of the temperature; the present results therefore present an opportunity of gaining further insight into the origin of differences in these values.

The dianionic ligands SO_3^{2-} and $\text{S}_2\text{O}_3^{2-}$, in their reactions with both ACCBs and ACSYCbs, produce positive ΔH values and, given the compensation effect mentioned above, ΔS values that are very large and positive. By contrast, the three mono-anionic ligands studied produce negative ΔH values and ΔS values that range from large and positive to moderately large and negative. To assess to what extent this effect is dependent on the desolvation of the dianion, required before coordination to the metal can occur, would need data, as yet not available, in other solvents, but we do note that the smaller SO_3^{2-} ion, with a smaller volume (216 Å³) and hence a higher charge density, produces a significantly larger ΔS value in its reaction with ACCBs than the larger, and hence more charge-diffuse, $\text{S}_2\text{O}_3^{2-}$ ion (274 Å³). Work in other solvents is planned and will be reported elsewhere.

For both ACCBs and ACSYCbs, the $\log K$ values for SO_3^{2-} are significantly larger than those for $\text{S}_2\text{O}_3^{2-}$; indeed, the latter coordinates ACSYCbs so poorly that we were unable to study the temperature dependence of the reaction because of the unreliability of the data. In general, SO_3^{2-} forms more stable complexes with hard and borderline metal ions than $\text{S}_2\text{O}_3^{2-}$, whereas the converse is true for soft metal ions.⁶ For example, $\log K$ [T (°C) = 25 °C; μ (M) = 0, unless otherwise indicated] for SO_3^{2-} with Mg^{2+} is 2.36 and with Fe^{III} is 6.6 (20; 0.5). For $\text{S}_2\text{O}_3^{2-}$, the values are 1.82 with Mg^{2+} and 2.09 (20; 0.1) with Fe^{III} . In the case of Co^{II} and Ni^{II} , the differences are smaller: SO_3^{2-} with Co^{II} has $\log K = 3.08$ and that with $\text{Ni}^{\text{II}} = 2.88$, whereas $\text{S}_2\text{O}_3^{2-}$ with $\text{Co}^{\text{II}} = 2.05$ and that with $\text{Ni}^{\text{II}} = 2.06$. For soft ions like Ag^{I} , $\log K = 5.6$ for SO_3^{2-} but 9.6 (25; 0.1) for $\text{S}_2\text{O}_3^{2-}$, and for Hg^{II} , $\log \beta_2 = 22.33$ (25; 0.5) for SO_3^{2-} but 29.23 for $\text{S}_2\text{O}_3^{2-}$. Thus, a $\log K$ (25 °C) value of 5.0 for SO_3^{2-} but only 0.5 for $\text{S}_2\text{O}_3^{2-}$ for substitution of H_2O in ACCBs is an indication of the generally hard nature of Co^{III} in this cobalt corrin. This is also true for ACSYCbs.

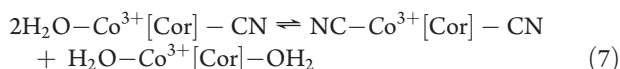
A comparison of the ΔH values obtained for the reactions of the ligands studied in this work with ACCBs and ACSYCbs highlights differences in the behavior of the metal ion in the two cobalt corrins toward the incoming ligand. The ligands that have a harder donor atom (N in N_3^- and NO_2^-) produce ΔH values that are more negative in the reactions with ACSYCbs than in the analogous reactions with ACCBs. If the donor atom is softer, however (C in CN^- and S in SO_3^{2-}), then ΔH is more negative

(or less positive) for the reaction with ACCBs than for the reaction with ACSYCbs. As indicated in the accompanying paper, the spectroscopic evidence indicates that Co^{III} is somewhat softer in ACCBs than in ACSYCbs; the present results indicate a preference of the softer metal center in ACCBs for softer ligands and the harder metal center in ACSYCbs for the harder ligands. Hence, the electronic structure of the equatorial ligand in cobalt corrins can modify the thermodynamics of the interaction between the metal and an axial ligand.

Reaction Kinetics. The substitution of coordinated H_2O in ACCBs and ACSYCbs shows biphasic kinetics, with k_2^{II} an order of magnitude smaller than k_1^{II} (Table 2). The biphasic kinetics could be due to the presence of diastereomers, each reacting with CN^- at a different rate, or to some other reaction. The difference between the rate constants for the substitution of H_2O by CN^- at the α and β faces is expected to be very small and not distinguishable by stop flow,³³ as has been found for ACCbi with CN^- .^{9,33,34} For the substitution of H_2O in aquahydroxocobinamide (AHCbi), which also exists as a pair of diastereomers with OH^- on either the α or β face, by the ligands CN^- , N_3^- , pyridine, *N*-methylimidazole, and 3-aminopropan-1-ol, only monophasic kinetics are observed; the second-order rate constant for substitution of the two diastereomers of AHCbi by CN^- is $2.3 \times 10^3 \text{ M}^{-1} \text{ s}^{-1}$ at pH 12.³⁵

For comparison, the second-order rate constants for the reaction of cyanide with the two faces of protonated base-off cyanocobalamin (with H_2O coordinated to Co) are $2.1 \times 10^6 \text{ M}^{-1} \text{ s}^{-1}$ (α face) and $2.9 \times 10^6 \text{ M}^{-1} \text{ s}^{-1}$ (β face).²⁰ For this reason and for further reasons described below, it appears unlikely that the observed biphasic kinetics are due to a difference in the reaction rate of the two diastereomers. The question of the origin of the biphasic kinetics then arises.

For ACCBs and ACSYC in solution, as has been observed for ACCbi,⁹ it appears that there is an equilibrium between the aquacyano species and the dicyano and diaqua species (eq 7).



For ACCBs, small amounts of DCCBs were seen in the UV-vis spectra (peak at $\sim 580 \text{ nm}$), TLC (purple spot at $R_f = 0.62$), HPLC ($R_t = 2.0 \text{ min}$), and column chromatography (see above). The presence of DACBs was inferred but not detected because its UV-vis spectrum is very similar to that of ACCBs and it gives a streak rather than a compact spot on TLC. Similarly, DCSYCbs in small amounts was seen in the UV-vis spectra of ACSYCbs (peak at $\sim 485 \text{ nm}$). Assuming that the $\text{p}K_a$ values of DACBs and aquahydroxocobester (AHCbs) are similar to those of DACbi (5.9) and AHCbi (10.3),^{8,10,35} respectively, at pH 9.6 the "DACBs" present in solution should actually consist of 83% AHCbs, which is labile to substitution by CN^- , and 17% dihydroxocobester (DHCbs), which is inert.^{10,34,35} Because the trans effect of OH^- is smaller than that of CN^- in cobalt corrin chemistry,^{10,35} the substitution of H_2O by CN^- trans to CN^- will be faster than that trans to OH^- (OH^- itself is inert to substitution by CN^-). We suggest, therefore, that the slower phase observed in the reactions of ACCBs and ACSYCbs with CN^- is due to the (unavoidable) presence of some AHCbs species in solution and the faster phase is the average rate of substitution of coordinated H_2O in the two diastereomers.

There is a related study on the kinetics of the reaction of ACCbi and CN^- .³⁴ Only the second-order rate constant

(25°C , $\mu = 0.2 \text{ M}$) was reported ($k^{\text{II}} = 2.1 \times 10^5 \text{ M}^{-1} \text{ s}^{-1}$), and the authors comment in a footnote that "although two isomers are present, their rates are indistinguishable". By contrast, Zelder et al.³⁶ also observed biphasic kinetics for the reaction with CN^- of the potassium salt of aquacyanocobyrinic acid (in which all of the $-\text{OCH}_3$ groups in aquacyanocobester are replaced by $-\text{O}^- \text{K}^+$ groups) and attributed the fast reaction to the diastereomer that has H_2O on the less sterically crowded face and the slow reaction to the diastereomer that has H_2O on the more sterically crowded face.

We examined the kinetics of the substitution of coordinated H_2O by CN^- in DACBs at pH 9.0 (and it is reasonable to assume that the predominant species in solution at this pH is AHCbs) and found that the change in absorbance at the monitoring wavelength, 367 nm, very nearly (but not quite) conformed to a single-exponential process (Figure S9 in the Supporting Information). We were unable to reliably fit the data with a double-exponential function because of the high cross-correlation of variables. Because AHCbs is also expected to exist as a mixture of two diastereomers, they clearly react at very similar rates. The apparent second order rate constant at 25°C is $5.3(5) \times 10^3 \text{ M}^{-1} \text{ s}^{-1}$; this is statistically identical with the value of $5.1 \times 10^3 \text{ M}^{-1} \text{ s}^{-1}$ obtained for the slow phase of the reaction of ACCBs with CN^- (Table S2 in the Supporting Information). While this does not prove that the slow phase is due to the presence of DACBs in the sample of ACCBs, it is certainly strong supporting evidence. We conclude that both diastereomers of each of ACCBs and ACSYCbs react at experimentally indistinguishable rates. We therefore use the value of k_1^{II} to compare the effect of the interrupted conjugation of the corrin on the rate of the substitution of coordinated H_2O , the key question in this work.

The rate of the reaction is too fast to observe the saturation kinetics required for an unequivocal determination of the mechanism,³⁷ but it is very likely that the reactions proceed through a dissociative interchange mechanism, as has been shown for aquacobalamin (substitution of H_2O trans to 5,6-dimethylbenzimidazole; see, for example, ref 38 and references cited therein) and AHCbi³⁹ (H_2O trans to OH^-).

The value of k_1^{II} is between 4.6 (at 5°C) and 2.6 (at 35°C) times smaller for substitution of H_2O by CN^- in ACSYCbs than in ACCBs; thus, the metal ion becomes more inert with a decrease in the extent of delocalization of the π -electron system. Assuming that the mechanism of the reaction is indeed a dissociative interchange mechanism, the second-order rate constant k_1^{II} is a composite rate constant, $k_1^{\text{II}} = k_1^i K^{\text{OS}}$, where K^{OS} is the equilibrium constant for the formation of an outer-sphere or encounter complex between cobalt corrin and incoming CN^- and k_1^i is the rate constant for the interchange of H_2O and CN^- between the inner and outer coordination spheres of the metal ion. From the Fuoss-Eigen model,⁴⁰ the value of K^{OS} is a function of the molar volume of the encounter complex (it is reasonable to expect this to be very similar for ACCBs + CN^- and for ACSYbs + CN^-) and an electrostatic term, which is controlled by the distance between the two reactants (again, expected to be very similar) and their charges (which are identical). Thus, variation in k_1^{II} is very likely to be due to variation in k_1^i and to reflect the inherent differences in the rate of interchange between the departing H_2O ligand and the incoming CN^- ligand.

The transition state for the reaction will consist of a $\text{Co}-\text{OH}_2$ bond, which is substantially elongated, and a $\text{Co}-\text{CN}$ bond,

which is beginning to form. The value of ΔH^\ddagger for the reaction of ACCbs with CN^- is smaller by nearly 12 kJ mol^{-1} than that for the reaction of the same ligand with ACSYCbs. This is consistent with a transition state that occurs earlier along the reaction coordinate and in which the extent of the bonding between the softer metal center of ACCbs and the ligand is greater than that in ACSYCbs with its harder metal center. If ΔS^\ddagger were invariant, this would make the reaction with the former corrin over 100 times faster than that with the latter at 25°C . However, the earlier transition state also means that departing H_2O and incoming CN^- are more constrained by their interaction with the metal. Consequently, ΔS^\ddagger is more negative by over $30 \text{ J K}^{-1} \text{ mol}^{-1}$, retarding the reaction by over 40 times. This compensation effect between ΔH^\ddagger and ΔS^\ddagger levels out and masks the very significant effect of the change in the electronic properties of the equatorial ligand on the rate of substitution of the axial ligand. In our view, the values of ΔH^\ddagger are the most informative (rather than those of k_1^{II}), and these indicate the very significant increase in inertness of Co^{III} upon a decrease in the extent of conjugation of the corrin ligand.

CONCLUSIONS

In this and the accompanying paper, we compared the physical and chemical properties of cobalt(III) in aquacyanocobester (ACCbs), which retains the 13-atom, 14π -electron system of normal cobalt corrins, with those in stable yellow aquacyanocobester (ACSYCbs), where oxidation at C5 leads to a less extensive conjugated system. The bands in the electronic spectrum of DCSYCbs are shifted to shorter wavelengths, which is consistent with a PBE1PBE/6-311G(d,p) density functional theory (DFT) calculation that shows that the HOMO–LUMO gap in DCSYCbs is larger than that in DCCbs. PBE1PBE/6-311G(d,p) DFT calculations show that while the d orbital population is very similar in DCCbs and in DCSYCbs, the d orbitals in the former span a significantly greater energy range (2.61 eV) than those in the latter (1.86 eV). The ^{59}Co resonance of DCSYCbs is shifted downfield from that in DCCbs; a comparison with available ^{59}Co data of cobalamins and cobaloximes indicates that CN^- interacts more strongly with the metal in DCCbs than that in DCSYCbs. As the strength of the interaction between Co^{III} and the equatorial macrocyclic ligand increases, the IR stretching of axially coordinated CN^- shifts to lower frequency ([14]ane N_4 > cobaloxime > porphyrin > corrin). Because ν_{CN} in DCSYCbs occurs at a higher frequency than that in DCCbs, the corrin in DCCbs interacts more strongly with the metal than the stable yellow corrin with its diminished conjugation. These results reveal that there is greater overlap between the corrin and the metal orbitals in DCCbs than in DCSYCbs, which gives the metal in the former a softer, more covalent character than that in the latter.

The substitution of H_2O by CN^- in the two cobesters proceeds with biphasic kinetics, and we argue that the faster process corresponds to the substitution of coordinated H_2O on both faces of the corrin because both faces are more or less equally sterically accessible. [The slower process, we believe, corresponds to the substitution of coordinated H_2O in AHCbs, present as an impurity in solution from the spontaneous reaction of the aquacyano species to form diaqua (or aquahydroxo) and dicyano species.] Co^{III} is more labile in ACCbs than in ACSYCbs, and the value of k_1^{II} , the second-order rate constant for the faster reaction, is between 4.6 (at 5°C) and 2.6 (at 35°C) larger.

Because the mechanism is likely to be a dissociative interchange mechanism, $k_1^{\text{II}} = K^{\text{OS}}k_1^{\text{I}}$, but K^{OS} is expected to be very similar for the two cobesters; differences in k_1^{II} indicate inherent differences in the rate of interchange between H_2O and CN^- on the metal. The value of ΔH^\ddagger for k_1^{II} is about 12 kJ mol^{-1} smaller for ACCbs than for ACSYCbs, which is consistent with a transition state that occurs earlier along the reaction coordinate and in which the extent of the bonding between the softer metal center of ACCbs and the ligand is greater than that in ACSYCbs with its harder metal center. This means that ACCbs is over 100 times more labile than ACSYCbs toward the substitution of coordinated H_2O by CN^- . The effect is masked, however, by a compensating decrease in ΔS^\ddagger , which is over $30 \text{ J K}^{-1} \text{ mol}^{-1}$ more negative. Diminishing the extent of the conjugation of the corrin ligand therefore causes a very significant increase in the inertness of Co^{III} . Thus, the fact that Co^{III} is so labile in the cobalamins is undoubtedly due, in part, to the labilizing cis effect of the corrin ligand.

ASSOCIATED CONTENT

S Supporting Information. Spectral changes, change in absorbance at 367 nm for the reaction of ACCbs, view of the upper (β) face of the MD/SA energy-minimized structures, fits of eqs 3 and 4 to the titration of ACSYCbs, weighted linear least squares fits to the van't Hoff relationship, plot of the pseudo-first-order rate constants k_1 and k_2 as a function of the cyanide concentration, Eyring plots of the second-order rate constants, relationship between ΔH and ΔS , and tables of pseudo-first-order rate constants and primary kinetic data. This material is available free of charge via the Internet at <http://pubs.acs.org>.

AUTHOR INFORMATION

Corresponding Author

*E-mail: Susan.Chemaly@wits.ac.za (S.M.C.), Helder.Marques@wits.ac.za (H.M.M.).

ACKNOWLEDGMENT

The financial assistance of the Department of Science and Technology and the National Research Foundation, Pretoria, through the South African Research Chairs Initiative, and the University of Witwatersrand, Johannesburg, is gratefully acknowledged. We thank R. Mampa for running the ^1H NMR spectrometer.

REFERENCES

- (1) Chemaly, S. M.; Brown, K. L.; Fernandes, M. A.; Munro, O. Q.; Grimmer, C.; Marques, H. M. *Inorg. Chem.* **2011**, accepted, doi: 10.1021/ic200285k.
- (2) Friedrich, W. Z. *Naturforsch. B* **1966**, *21*, 595–596.
- (3) Pratt, J. M. *The Inorganic Chemistry of Vitamin B12*; Academic Press: London, 1972.
- (4) Friedrich, W.; Bieganowski, R. Z. *Naturforsch. B* **1967**, *22*, 741–747.
- (5) Friedrich, W.; Ohlms, H.; Sandeck, W.; Bieganowski, R. Z. *Naturforsch. B* **1967**, *22*, 839–850.
- (6) Martell, A. E.; Smith, R. M.; Motekaites, R. J. *NIST Critically Selected Stability Constants of Metal Complexes*, version 8.0; NIST: Gaithersburg, MD, 2004.
- (7) Marques, H. M.; Bradley, J. C.; Brown, K. L.; Brooks, H. *Inorg. Chim. Acta* **1993**, *209*, 161–169.

- (8) Broderick, K. E.; Singh, V.; Zhuang, S.; Kambo, A.; Chen, J. C.; Sharma, V. S.; Pilz, R. B.; Boss, G. R. *J. Biol. Chem.* **2005**, *280*, 8678–8685.
- (9) Betterton, E. A. Ph.D. Thesis, The University of Witwatersrand, Johannesburg, South Africa, 1982.
- (10) Baldwin, D. A.; Betterton, E. A.; Pratt, J. M. *J. Chem. Soc., Dalton Trans.* **1983**, 217–223.
- (11) Hamza, M. S. A. *Personal communication*.
- (12) Allinger, N. L.; Yuh, Y. H.; Lii, J. H. *J. Am. Chem. Soc.* **1989**, *111*, 8551–8556.
- (13) *HyperChem*, 7.05; Hypercube Ltd.: Gainesville, FL.
- (14) Marques, H. M.; Brown, K. L. *THEOCHEM* **1995**, *340*, 97–124.
- (15) Marques, H. M.; Brown, K. L. *Coord. Chem. Rev.* **2002**, *225*, 123–158.
- (16) Stewart, J. J. P. *J. Comput. Chem.* **1989**, *10*, 209–220.
- (17) Bodor, N.; Gabanyi, Z.; Wong, C. J. *J. Am. Chem. Soc.* **1989**, *111*, 3783.
- (18) Gavezotti, A. *J. Am. Chem. Soc.* **1983**, *10*, 5220.
- (19) Ford, S. H.; Nichols, A.; Gallery, J. M. *J. Chromatogr. A* **1991**, *536*, 185–191.
- (20) Reenstra, W. W.; Jencks, W. P. *J. Am. Chem. Soc.* **1979**, *101*, 5780–5791.
- (21) Johnson, G. D.; Bowen, R. E. *J. Am. Chem. Soc.* **1965**, *87*, 1655.
- (22) *SigmaPlot*, 11.0; Systat Software, Inc.: San Jose, CA, 2008.
- (23) Marques, H. M.; Munro, O. Q.; Crawcour, M. L. *Inorg. Chim. Acta* **1992**, *196*, 221–229.
- (24) Firth, R. A.; Hill, H. A. O.; Mann, B. E.; Pratt, J. M.; Thorp, R. G.; Williams, R. J. P. *J. Chem. Soc. A* **1968**, 2419–2428.
- (25) Zhou, K.; Zelder, F. *Eur. J. Inorg. Chem.* **2011**, 53–57.
- (26) Butler, P. A.; Murtaza, S.; Krätler, B. *Monatsh. Chem.* **2006**, *137*, 1579–1589.
- (27) Randaccio, L.; Furlan, M.; Geremia, S.; Šlouf, M. *Inorg. Chem.* **1988**, *37*, 5390–5393.
- (28) Perry, C. B.; Fernandes, M. A.; Brown, K. L.; Zou, X.; Valente, E. J.; Marques, H. M. *Eur. J. Inorg. Chem.* **2003**, 2095–2107.
- (29) Garau, G.; Geremia, S.; Marzilli, L. G.; Nardin, G.; Randaccio, L.; Tauzher, G. *Acta Crystallogr., Sect. B* **2003**, 51–59.
- (30) Randaccio, L.; Geremia, S.; Nardin, G.; Šlouf, M.; Srnova, I. *Inorg. Chem.* **1999**, *38*, 4087–4092.
- (31) Randaccio, L.; Geremia, S.; Stener, M.; Toffoli, D.; Zangrando, E. *Eur. J. Inorg. Chem.* **2002**, 93–103.
- (32) Hamza, M. S. A. *J. Inorg. Biochem.* **1998**, *69*, 269–274.
- (33) Bernasconi, C. F. *Relaxation Kinetics*; Academic Press: New York, 1976.
- (34) Baldwin, D. A.; Betterton, E. A.; Pratt, J. M. *S. Afr. J. Chem.* **1982**, *35*, 173–175.
- (35) Marques, H. M.; Bradley, J. C.; Brown, K. L.; Brooks, H. *J. Chem. Soc., Dalton Trans.* **1993**, 3475–3478.
- (36) Männel-Croisé, C.; Probst, B.; Zelder, F. *Anal. Chem.* **2009**, *81*, 9493–9498.
- (37) Meier, M.; van Eldik, R. *Inorg. Chem.* **1993**, *32*, 2635–2639.
- (38) Knapton, L.; Marques, H. M. *Dalton Trans.* **2005**, 889–895.
- (39) Marques, H. M.; Bradley, J. C.; Campbell, L. A. *J. Chem. Soc., Dalton Trans.* **1992**, 2019–2027.
- (40) Douglas, B. E.; McDaniel, D. H.; Alexander, J. J. *Inorganic Chemistry*, 2nd ed.; John Wiley & Sons, Inc.: New York, 1980.